Scientia Iranica, Vol. 14, No. 5, pp 450–457

SCIENTIA IRANICA

An Energy-Based Paradigm for Reliability Assessment Caused by Creep Damage in Axisymmetric Components

K. Zarrabi* and L. Ng Kiam Yam[1]

The creep of materials is a research topic of major significance in the life assessment and design of many pressure components used in various industries, such as power generation plants and chemical plant refineries. Often, these components are axisymmetric, both in terms of geometry and loading. To predict the creep life of such components, one necessary ingredient is a creep damage paradigm. The current creep damage paradigms are either too cumbersome to be readily employed and/or not sufficiently accurate for practical applications. This paper describes a creep damage paradigm that alleviates the major shortcomings of the existing paradigms, yet is simple enough to be readily applicable to industrial cases. Comparison with experimental data shows that the paradigm is capable of predicting creep life with an accuracy of 14% or better.

INTRODUCTION

There are several mechanisms by which a loaded engineering component operating within a creep regime may fail, such as, gross creep deformation/creep rupture, creep deformation enhanced by cyclic loading, creep damage in the presence of corrosion, fatigue, elastic fracture, etc. The present work will concentrate on a pragmatic engineering damage paradigm for cases where the gross creep damage is dominant under constant loading and uniform temperature and will study the problem from the macroscopic (engineering) point of view and not from the microscopic (material science) point of view. An account of various mechanisms of microscopic creep damage is presented elsewhere; see, for example [1].

One of the simplest and most employed creep damage paradigms is the Robinson time fraction rule [2]:

$$\sum_{i=1}^{n} \frac{\Delta t_i(\sigma_r)}{t_{ri}(\sigma_r)} = 1, \tag{1}$$

where $\Delta t_i(\sigma_r)$ is the ith time interval and is a function of the rupture stress, σ_r, and $t_{ri}(\sigma_r)$ is the time-to-rupture for the ith time interval that is also a function of σ_r. The rupture stress is the stress component that is responsible for creep damage and it is taken to be a function of the principal stress, σ_1, (causing creep cavitation) and the effective stress, σ, (causing dislocation glide and/or grain boundary sliding) usually as [3,4]:

$$\sigma_r = \alpha\sigma_1 + (1 \quad \alpha)\sigma, \tag{2}$$

where α is a material parameter whose value depends on the temperature and is not known a priori. This may be a major limitation of the time fraction damage paradigm. It is worth noting that there are other equations for expressing σ_r, in terms of the principal, effective and hydrostatic stresses [4]. All of these equations contain one or more material parameter, whose values are not known a priori and whose evaluations may not be economical in practice.

Another creep damage paradigm is based on the continuum damage mechanics that were originally proposed by Kachanov and Rabotnov [5,6]. This paradigm will be referred to as KR-CDM in this paper. KR-CDM represents a significant step forward in finding an engineering solution for the complex creep damage problem. Kachanov/Rabotnov used a scalar parameter (D) to represent creep damage [7] and modified Kachanov/Robotnov's paradigm to predict the creep deformation and rupture more accurately. Hayhurst also proposed that the damage should be

*. *Corresponding Author, School of Mechanical and Manufacturing Engineering, The University of New South Wales, Sydney, NSW 2052, Australia.*

1. *School of Mechanical and Manufacturing Engineering, The University of New South Wales, Sydney, NSW 2052, Australia.*

a tensor and used two parameters to model creep damage [7]. Fundamentally, KR-CDM is based on the following coupled equations:

$$\dot{\varepsilon}^c = \dot{\varepsilon}_0^c \left[\frac{\sigma}{\sigma_{0(1\quad D)}}\right]^n, \tag{3}$$

$$\dot{D} = \dot{D}_0 \left[\frac{\sigma}{\sigma_{0(1\quad D)}}\right]^v, \tag{4}$$

where $\dot{\varepsilon}^c$ is the equivalent creep strain rate, $\dot{\varepsilon}_0^c$ is the equivalent creep strain rate at a reference effective stress, σ_0, $\dot{D}$ is the damage rate, $\dot{D}_0$ is the damage rate at the reference stress, σ_0, n is the creep stress index and v is a material parameter. It is assumed that $D = 0$ at $t = 0$ and $D = D_r$ when $t = t_r$, where t_r is time-to-rupture. Usually, D_r is taken to be unity but, in practice, it may not be so. The other limitation of KR-CDM is that the pertinent material data are often not readily available. Furthermore, the calibration of the paradigm, especially when the damage is taken to be a tensor, is tedious and time-consuming. Also, to date, KR-CDM has not been incorporated in most commercial finite element computer codes and, therefore, is not readily applicable to practical cases, where the practicing engineer has limited time to predict the creep life of an industrial component. Another major problem is that, in KR-CDM, the damage is coupled with σ only and the effects of σ_1 on the damage are ignored, which is strictly not correct.

There are other creep damage paradigms, but, for the sake of brevity, they are not described here. For more details, see, for example [1,8]. In summary, the existing creep damage paradigms are either not sufficiently accurate and/or the required data are not readily available for pragmatic engineering applications and, hence, the proposed paradigm.

PROPOSED CREEP PARADIGM

Consider a defect-free component. The paradigm allows the material to undergo elastic-creep deformation, therefore, the dominant damage mechanism is creep and, at the point of failure, the component fails by excessive creep deformation and/or creep rupture. Consider a component that is subjected to several mechanical loads that, taken together, constitute a set: $\{F\} = \{F_1, F_2, \cdots F_n\}$. These loads are increased in their respective magnitudes from zero to their operational levels, $\{F_0\}$, over relatively short periods of time, so that it can be assumed that, at $t = 0$, they instantly cause elastic deformation. Having reached their respective operational levels, the loads are taken to be constant until the point of failure. The component is also subjected to a constant and uniform material temperature. As time progresses, the material undergoes creep deformation. The paradigm assumes that the creep damage induced in the material (D) is proportional to the average internal energy (W) absorbed within a damaged zone of volume, V_D, by the material. Also,

$$W = W_s + \frac{\{F_0\}\quad\{F\}}{\{F_0\}} W_t, \tag{5}$$

where W_s is the average internal energy in the damaged zone due to mechanical loads, i.e., strain energy and W_t is the average internal (thermal) energy in the absence of stress in the damaged zone. The paradigm postulates that, under normal operational stresses/strains where $\{F\} = \{F_0\}$, W_s is the dominant term in Equation 5 and $W \approx W_s$. As the stresses/strains approach zero, W_t becomes the dominant term in Equation 5 and $W \approx W_t$. In addition, the damage zone is taken to be the entire cross-section of the axisymmetric component; (see the next section for verification of these assumptions). In the following, the superscript, e, refers to elastic and c refers to creep. At time t, the rate of the total internal energy per unit of volume (i.e., the internal energy density rate), $d\dot{W}$, is the sum of the rates of elastic internal energy per unit of volume, $d\dot{W}^e$, and creep internal energy per unit of volume, $d\dot{W}^c$. Thus:

$$d\dot{W} = d\dot{W}^e + d\dot{W}^c. \tag{6}$$

This may be expressed in terms of stress (σ_{ij}) and strain rate ($\dot{\varepsilon}_{ij}^k$) components, as follows:

$$d\dot{W} = \sigma_{ij}(\dot{\varepsilon}_{ij}^e + \dot{\varepsilon}_{ij}^c) + \frac{\{F_0\}\quad\{F\}}{\{F_0\}} \dot{W}_t. \tag{7}$$

The average total internal energy within the damaged zone of volume V_D can be calculated by integrating Equation 7, with respect to volume and time:

$$W = \frac{1}{V_D}\int\int\{[\sigma_{ij}(\dot{\varepsilon}_{ij}^e + \dot{\varepsilon}_{ij}^c)]dV\}dt + \frac{\{F_0\}\quad\{F\}}{\{F_0\}} W_t. \tag{8}$$

To compute W using Equation 8, first, the stress and strain components, as a function of time, should be calculated up to the rupture time. For simple problems, this may be achieved analytically and, for more complex cases, a numerical method, such as the Finite Element Method (FEM), may be employed. In determining the stress and strain fields as functions of time, creep constitutive relationships are used. These data are part of the essential ingredients of any creep analysis and obtained from the uniaxial creep tests. If no direct material data are available, published generic data may be utilized, with appropriate sensitivity analyses to cover the uncertainties. Using Equation 8, W, as a function of time, is computed. Then, the

paradigm proposes to modify the time fraction rule and assumes that the creep rupture occurs when:

$$\sum_{i=1}^{n} \frac{\Delta t_i(W)}{t_{ri}(W)} = 1. \tag{9}$$

To calculate creep life, the expression for the uniaxial internal energy is also needed. This expression depends on the creep constitutive equation, e.g., for the Norton power law, for the non-zero operational stress/strain levels ($W_t \approx 0$):

$$W = B\sigma^{(n+1)} t_r + \frac{\sigma^2}{2E}, \tag{10}$$

where B is the Norton stress coefficient and E is the modulus of elasticity. Other terms have previously been defined. Note that the relationship between σ and t_r in Equation 10 is also known from the uniaxial rupture data, so that:

$$\sigma = f(t_r). \tag{11}$$

Combining Equations 10 and 11 gives:

$$W = B[f(t_r)]^{(n+1)} t_r + \frac{[f(t_r)]^2}{2E}. \tag{12}$$

The algorithm for creep life calculations will then be, as follows:

(a) Calculate $W = W(t)$ analytically or by FEM using Equation 8;

(b) Select sufficiently small time intervals, Δt_i;

(c) For each time interval, calculate W from Step a;

(d) Using W from Step c and the uniaxial data (Equation 12), calculate t_{ri};

(e) Compute $D = \sum \frac{\Delta t_i(W)}{t_{ri}(W)}$. If $D = 1$, then, take $t_r = \sum \Delta t_i$, otherwise, go to Step c and repeat the calculations for the next time interval.

Note that in the above algorithm there is no need to determine σ_r yet, as the paradigm allows for contributions to the creep damage from various stress components.

VERIFICATION

To evaluate the proposed paradigm, the experimental data from Brown [9] and Kwon et al. [10] were used. The experimental data in [9] were obtained from tests on thick and thin tubes and those described in [10] were obtained using notched bars. Evaluation of the proposed paradigm using each of these components is described below. In what follows, the MSC.MARC finite element code [11] was employed using 6-node triangular axisymmetric elements for each finite element analysis.

Thick Tube

The thick tube had an internal diameter of 20 mm, external diameter of 40 mm and was subjected to a uniform internal pressure of 106.67 MPa and a uniform temperature of 565°C. Its material was 0.5% Cr0, 5% Mo and 0.25% V steel, with the modulus of elasticity at the test temperature of $E = 0.1542 \times 10^6$ MPa. Also, $n = 11.98$ and $B = 6.1033 \times 10^{-33}$, where these values gave time in hours and stress in MPa. The uniaxial creep rupture data was described by:

$$\sigma = -57.774 \log t_r + 367.79. \tag{13}$$

The tests resulted in an average experimental tube life of 9,000 hours. To apply the creep damage paradigm and algorithm, described in the previous section, to the thick tube, it was analyzed using the 1000 6-node axisymmetric triangular elements and its finite element mesh is shown in Figure 1. Because of symmetry, half of the length of the tube was modeled imposing symmetry conditions at one end and applying a uniform axial traction of 35.56 MPa at the opposite end to simulate the end pressure loading. A uniform internal pressure of 106.67 MPa was applied to the inner face of the model in the radial direction.

The computed tangential and von Mises effective stresses versus radial distance at various time points are plotted in Figures 2 and 3, respectively.

Using the finite element results and Equation 8 and noting that, at operational pressure, the second term in Equation 8 vanishes, the average strain energy across a tube section (the damaged zone) was computed, as follows:

$$W = 4 \times 10^{-13} t^3 - 3 \times 10^{-8} t^2 + 1 \times 10^{-4} t + 0.1586, \tag{14}$$

where W is in Nmm/mm^3 and t is in hours. Using the data described in this section and in the algorithm of the previous section, the creep life of the tube was predicted as 8,840 (see Table 1).

Thin Tube

The thin tube had an internal diameter of 33.40 mm, external diameter of 40 mm and subjected to a uniform

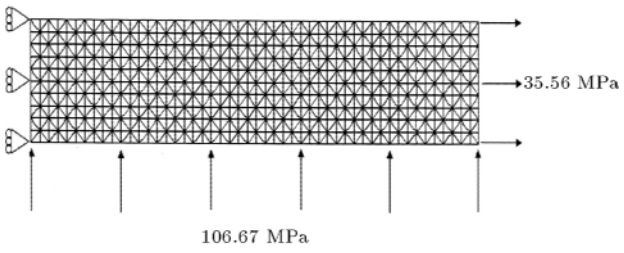

Figure 1. Finite element mesh of the thick tube.

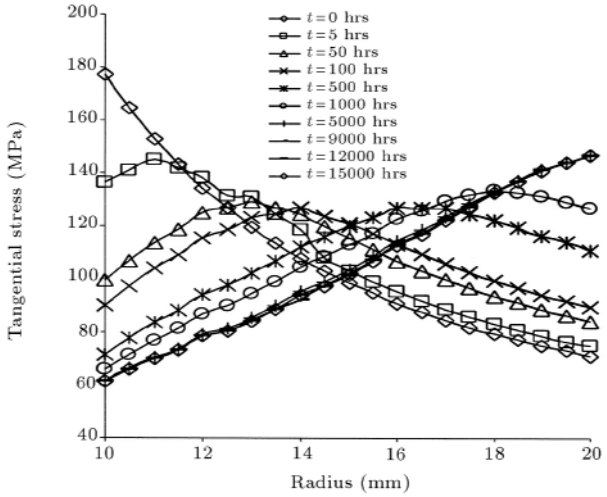

Figure 2. Tangential stress versus radial distance at various time points for the thick tube.

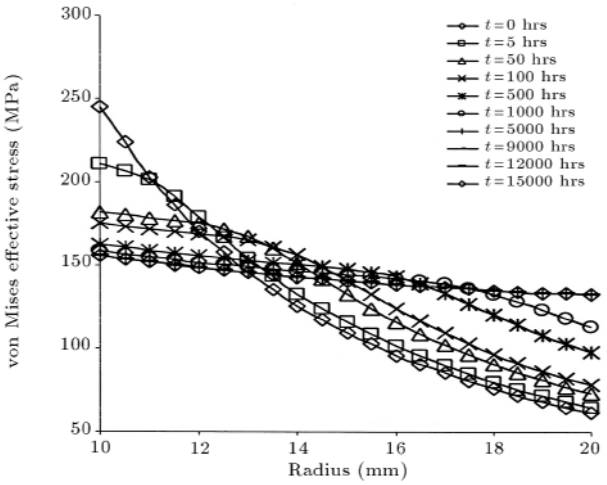

Figure 3. von Mises effective stress versus radial distance at various time points for the thick tube.

Table 1. Comparison of the experimental and predicted lives of the tubes

	Thick Tube	Thin Tube
Method	**Life (Hours)**	**Life (Hours)**
Experimental	9,000	5,000
Proposed paradigm	8,840	4,974
Error (%)	1.78	0.52

internal pressure of 28.77 MPa. Also, its material and temperature were the same as for the thick tube. The tests resulted in an average experimental tube life of 5,000 hours. Similar to the analysis of the previous section with the title of "Thick Tube", to apply the creep damage paradigm and algorithm, described previously, to the thin tube, it was analyzed using 2000 6-node axisymmetric triangular elements. The mesh, boundary conditions and computed stress patterns were similar to those of the thick tube and, for the sake of brevity, they are not depicted here. Using the finite element results and Equation 8 and noting that at the operational pressure, the second term in Equation 8 vanishes, the average strain energy across a tube section (the damaged zone) was computed, as follows:

$$W = 5 \times 10^{-11} t^3 - 2 \times 10^{-7} t^2 + 3 \times 10^{-3} t + 0.0792, \quad (15)$$

where W is in Nmm/mm^3 and t is in hours. Using the data described in this section and the algorithm represented in the previous section of "Proposed Creep Paradigm", the creep life of the thin tube was predicted as 4,974 hours (see Table 1).

Notched Bars

There were four different notched bars. The nominal geometry and dimensions of the bars were the same, but they differed in the details of the notch. The notched bars were:

(i) A bar with the modified British standard notch, as shown in Figure 4,

(ii) A bar with the Bridgman notch, as shown in Figure 5,

(iii) A bar with the modified Bridgman I notch, as shown in Figure 6,

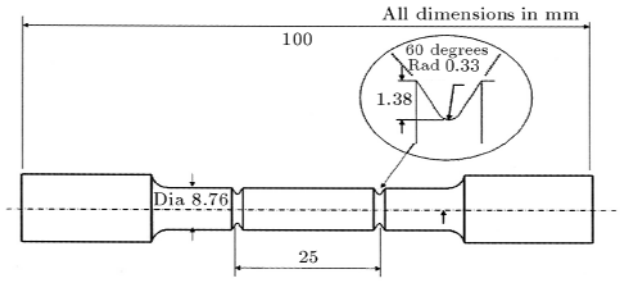

Figure 4. Bar with the modified British standard notch.

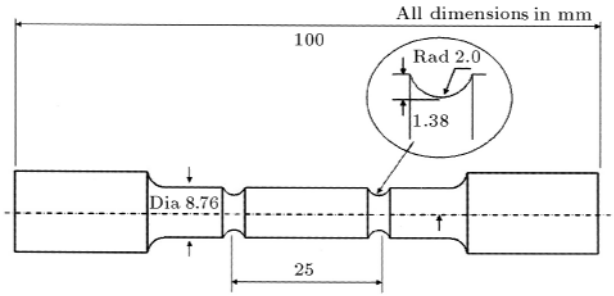

Figure 5. Bar with the Bridgman notch.

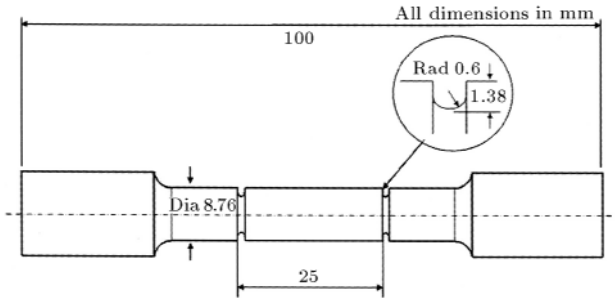

Figure 6. Bar with the modified Bridgman I notch.

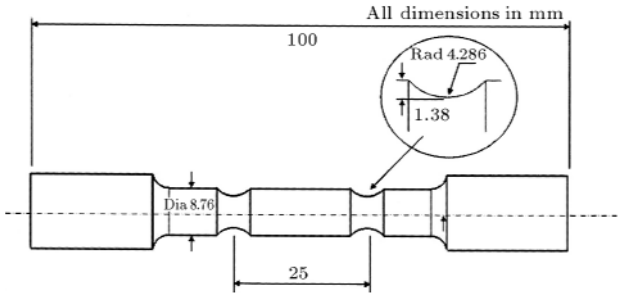

Figure 7. Bar with the modified Bridgman II notch.

(iv) A bar with the modified Bridgman II notch, as shown in Figure 7 (for more details regarding these notched bars, see [10]).

All bars were made of 2.25%Cr1%Mo steel and were subjected to a uniform temperature of 550°C, resulting in a modulus of elasticity of $E = 0.157 \times 10^6$ MPa, and creep properties of: $n = 9.0$, $B = 6.408 \times 10^{-24}$ (1/hour)/MPa^n, with uniaxial creep rupture properties of:

$$\sigma = (t_r/2.183x10^{20})^{(-1/7.9)}. \tag{16}$$

The finite element models of the bars were similar and, therefore, for the sake of brevity, the mesh and stress distributions for the bar with the modified British standard notch are shown in the next section as typical examples.

Bar-Modified British Standard Notch

The finite element model is shown in Figure 8. Because of symmetry, only half of the length of the bar was modeled. The mesh consisted of 3600 6-node axisymmetric triangular elements and the loading was a uniform axial traction of 94.76 MPa. The tests resulted in an average experimental life of 753 hours. The computed axial and von Mises effective stresses are plotted in Figures 9 and 10, respectively.

Using the finite element results and Equation 8 and noting that, at the applied load, the second term in Equation 8 vanishes, the average strain energy

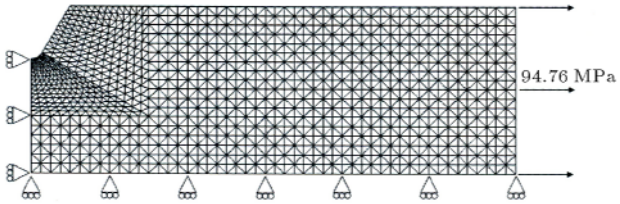

Figure 8. Finite element mesh of the bar with the modified British standard notch.

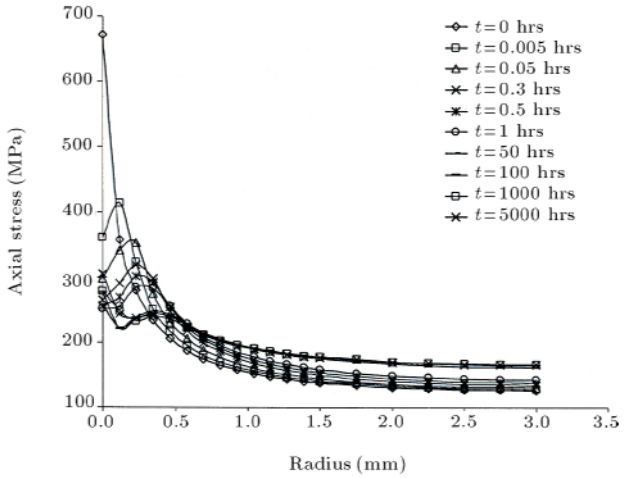

Figure 9. Axial stress versus radial distance at the notch root section for various time points for the bar with the modified British standard notch.

across the notch root section (the damaged zone) was computed, as follows:

$$W = 2\times10^{-7}t^3 - 1\times10^{-5}t^2 + 1.06\times10^{-2}t + 0.2442, \tag{17}$$

where W is in Nmm/mm^3 and t is in hours. Using the above data and the algorithm in the previous section, the creep life of the bar was predicted as 831 hours (see Table 2).

Bar-Bridgman Notch

The mesh consisted of 2250 6-node axisymmetric triangular elements and the loading was a uniform axial traction of 80.22 MPa. The tests resulted in an average experimental life of 3,899 hours. Using the finite element results and Equation 8 and noting that, at the applied load, the second term in Equation 8 vanishes, the average strain energy across the notch root section (the damaged zone) was computed, as follows:

$$W = 2\times10^{-9}t^3 - 4\times10^{-6}t^2 + 0.0059t + 0.1491, \tag{18}$$

where W is in Nmm/mm^3 and t is in hours. Using the above data described and the algorithm represented in the previous section, the creep life of the bar was predicted as 3,860 hours (see Table 2).

Table 2. Comparison of the experimental and predicted lives of the notched bars.

	Modified British Standard Notch ($K_t = 3.33$)	Bridgman Notch ($K_t = 1.61$)	Modified Bridgman I Notch ($K_t = 2.44$)	Modified Bridgman II Notch ($K_t = 1.38$)
Method	**Life (Hours)**	**Error (%)**	**Life (Hours)**	**Error (%)**
Experimental	753	3,899	1,041	4,933
Proposed paradigm	831	3,860	1,152	4,282
Error (%)	-10.36	1.00	-10.66	13.20

Note: K_t is the elastic stress concentration factor at the notch root.

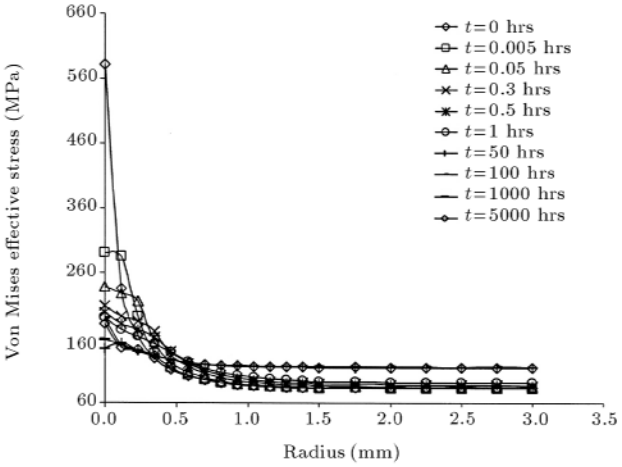

Figure 10. von Mises effective stress versus radial distance at the notch root section for various time points for the bar with the modified British standard notch.

Bar-Modified Bridgman I Notch

Because of symmetry, only half of the length of the bar was modeled for the finite element analysis. The mesh consisted of 2136 6-node axisymmetric triangular elements and the loading was a uniform axial traction of 91.48 MPa. The tests resulted in an average experimental life of 1,041 hours. Using the finite element results and Equation 8 and noting that, at the applied load, the second term in Equation 8 vanishes, the average strain energy across the notch root section (the damaged zone) was computed, as follows:

$$W = 1 \times 10^{-7} t^3 - 4 \times 10^{-5} t^2 + 8.7 \times 10^{-3} t + 0.1993, \tag{19}$$

where W is in Nmm/mm^3 and t is in hours. Using the above data and the algorithm described in the previous section, the creep life of the bar was predicted as 1,152 hours (see Table 2).

Bar-Modified Bridgman II Notch

Because of symmetry, only half of the length of the bar was modeled for the finite element analysis. The mesh consisted of 2136 6-node axisymmetric triangular elements and the loading was a uniform axial traction of 72.72 MPa. The tests resulted in an average experimental life of 4,933 hours. Using the finite element results and Equation 8 and noting that, at the applied load, the second term in Equation 8 vanishes, the average strain energy across the notch root section (the damaged zone) was computed, as follows:

$$W = 7 \times 10^{-10} t^3 - 2 \times 10^{-6} t^2 + 7.7 \times 10^{-3} t + 0.1169, \tag{20}$$

where W is in Nmm/mm^3 and t is in hours. Using the above data described and the algorithm represented in the previous section, the creep life of the bar was predicted as 4,282 hours (see Table 2).

RESULTS AND DISCUSSION

The stress distributions for the tubes typified the creep behavior of the 0.5%Cr0.5%Mo0.25%V steel at 565°C, i.e., initially, the stresses were higher at the inner surface and redistributed from the inner surface to the outer surface with creep deformation. Referring to Table 1, the maximum difference between the predicted and experimental creep lives of the tubes was 1.78%, indicating that the assumptions stated in the section of "Proposed Creep Paradigm" were justified. The creep life error was less for the thin tube compared with that for the thick tube. This might be due to the more accurate experimental data, although the accuracy of measurements was not specified in [9].

Considering the notched bars, as might be expected, the elastic stresses at the notch roots were initially high and then redistributed across the notch section with time, due to creep deformation. Referring to Table 2, the creep lives of the bars with the Bridgman (the elastic stress concentration factor at the notch root of $K_t = 1.61$) and modified Bridgman II ($K_t = 1.38$) notches were conservatively predicted, with an error of less than 14%. The creep lives of the bars with the modified British standard ($K_t = 3.33$) and modified Bridgman I ($K_t = 2.44$) notches, with an error of less than 11%, but, they were non-conservative. This may be due to: (a) Damage being

concentrated closer to the notch, due to the high value of K_t, causing the damaged zone to be less than the entire notch root section and/or (b) Inaccuracy, associated with creep testing. Kwon et al. from which the experimental data of the notched bars were obtained, do not state the accuracy of their results. To investigate the cause (a) the damage zones for bars with the modified British standard and modified Bridgman I notches were reduced until the predicted lives matched the respective experimental lives. For the bar with the modified British standard notch, this reduced the damage zone diameter in the notch root section from 6 mm to 5.75 mm, i.e., a reduction in diameter of 4.17%. For the bar with the modified Bridgman I notch, this reduced the damage zone diameter in the notch root section from 6 mm to 5.86 mm, i.e., a reduction in diameter of 2.33%. This may be explained as follows. As the notch becomes sharper, the stresses/strains and internal energy causing damage are concentrated closer to the notch root and the damage zone reduces. However, noting the complexity of high temperature creep testing, it is also likely that the experimental creep lives contain an error of more than 14%. Further testing and research is currently in progress to clarify this matter. Meanwhile, one may conservatively apply a factor of safety and reduce the predicted creep lives, using the proposed paradigm, by 14-15%. Noting that the current practice is to apply a safety factor of 200% or higher, the proposed paradigm is a significant improvement for predicting the creep lives of high temperature components.

CONCLUSIONS

The proposed new paradigm has several advantages over the existing creep damage paradigms. At a fundamental level, the experimental evidences have shown that the creep damage should be a multiaxial paradigm and the proposed paradigm takes into account the contributions from all the stress/strain components. The proposed paradigm is based on the exhaustion of the average total internal energy in the highly stressed/strained zone in the material. This is a measure of total deformation, as well as internal loading, in the component and, therefore, it should be the most appropriate for characterizing gross creep damage. In practical terms, the paradigm does not require quantities, such as the rupture stress (σ_r) and some material parameters that are cumbersome to determine and/or employ in practice. Therefore, the proposed paradigm should be more practical and should result in more accurate predictions for the creep life of components. Another advantage of the proposed paradigm is that it is simple, can be used in conjunction with any commercial finite element code with creep analysis capabilities and does not need finite element software modifications, as required by KR-CDM. It is shown that the proposed paradigm is capable of predicting creep lives with an accuracy of 14% or better.

NOMENCLATURE

B, n, α, v	material property
E	Young's Modulus
T	temperature
σ	effective stress
σ_{ij}	stress tensor
σ_r	rupture stress
σ_0	nominal effective stress
σ_1	major principal stress
ε_{ij}	strain tensor
ε^e_{ij}	elastic strain tensor
ε^c_{ij}	creep strain tensor
$\dot{\varepsilon}^c$	effective creep strain rate
$\dot{\varepsilon}^c_0$	effective creep strain rate at a nominal effective stress
D	creep damage parameter
$\dot{D}_0$	damage rate at the nominal stress
D_r	creep damage at rupture time
W	internal energy parameter
W_s	average internal (strain) energy
W_t	average internal (thermal) energy
$d\dot{W}$	internal energy density rate
$d\dot{W}^e$	elastic internal energy density rate
$d\dot{W}^c$	creep internal energy density rate
V_D	creep damage volume
F_0	operational load
t	time
t_r	time to rupture
Δt_i	small time step intervals

REFERENCES

1. Evans, H.E., *Mechanisms of Creep Fracture*, UK, Elsevier Applied Science (1984).
2. Robinson, E.L., *Trans. Am Soc. Mech. Eng.*, **74**, pp 777 (1952).
3. Penny, R.K. and Marriott, D.L., *Design for Creep*, London, Chapman & Hall, 2nd Edition (1995).
4. Webster, G.A., Holdsworth, S.R., Loveday, M.S., Perrin, I. and Purper, H. "A code of practice for conducting notched bar creep rupture tests and for interpreting the data", *European Structural Integrity Society*, Report ESIS TC11 (2001).

5. Kachanov, L.M., Izv Akad Nauk, *SSSR, Ser Fiz*, **8**, pp 26-31 (1958).

6. Rabotnov, Y.N., *Proc XII IUTAM Congress*, Stamford, CN, Eds: Hetenyi & Vincent, Springer, p 137 (1969).

7. Hayhurst, D.R. "The use of continuum damage mechanics in creep analysis for design", published in *Creep of Materials and Structures*, Hyde, T.H., Ed., UK, Mechanical Engineering Publications, pp 75-83 (1994).

8. Milne, I., Ritchie, R.O. and Karihaloo, B. "Comprehensive structural integrity", *Creep and High-Temperature Failure*, **5**, Volume Editor: Saxena A, London, UK, Elsevier Pergamon (2003).

9. Brown, R.J. "Creep rupture testing of tubular model", published in *Techniques for Multiaxial Creep Testing*, by Gooch, D.J. and How, I.M., London Elsevier Applied Science, pp 311-332 (1985).

10. Kwon, O., Thomas, C.W. and Knowles, D. "Multiaxial stress rupture behavior and stress-state sensitivity of creep damage distribution in Durhete 1055 and 2.25Cr1Mo steel", *Int. J. of Pressure Vessels and Piping*, **81**(6), pp 535-542 (2004).

11. MSC/MARC, *User Guide for Non-Linear Creep Analysis*, MSC. Software Corporation, USA (2005).